Asian Journal of Chemistry; Vol. 31, No. 2 (2019), 337-342

ASIAN JOURNAL OF CHEMISTRY

https://doi.org/10.14233/ajchem.2019.21608

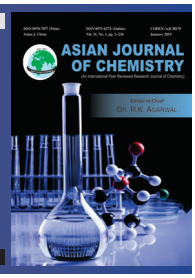

A Robust Modification of SiO_2 Nanoparticles by Poly(2-hydroxyethylmethacrylate) *via* Surface-Initiated Atom Transfer Radical Polymerization

DUY TRINH NGUYEN[1], THUONG NHAN PHU NGUYEN[1], DUY CHINH NGUYEN[1], VAN THI THANH HO[2], MD. RAFIQUL ISLAM[3], KWON TAEK LIM[3] and LONG GIANG BACH[1,*]

[1]Nguyen Tat Thanh University, 300A Nguyen Tat Thanh, District 4, Ho Chi Minh City, Vietnam
[2]Hochiminh University of Natural Resources and Environment, 236B Le Van Sy, Ward 1, Tan Binh District, Ho Chi Minh City, Vietnam
[3]Pukyong National University, Busan 608-737, Republic of Korea

*Corresponding author: Fax :+ 84 28 39404759, Tel : + 84 96 9294297; E-mail: blgiangntt@gmail.com

Received: 24 July 2018; *Accepted*: 25 September 2018; *Published online*: 31 December 2018; AJC-19205

An effortless and efficient method for the alteration of SiO_2 nanoparticles by poly(2-hydroxyethylmethacrylate) (PHEMA) has been developed. Initially, a strategic atom transfer radical polymerization (ATRP) initiator was anchored to SiO_2 nanoparticles surface *via* coupling reaction followed by surface-initiated atom transfer radical polymerization of HEMA successfully afforded chemically grafted PHEMA to SiO_2 nanoparticles (PHEMA-*g*-SiO_2). We used XPS, FT-IR and EDS analyses for confirming the covalent immobilization of PHEMA onto SiO_2 nanoparticles. TGA/DSC and zeta potentials measurements were used for determining the thermal and surface charge features of the nanocomposites, respectively.

Keywords: Surface functionalization, SiO_2 Nanoparticles, Polymer chains, Poly(2-hydroxyethylmethacrylate).

INTRODUCTION

There is a growing interest from modern fields such as electronics, optical, biomedicine and renewable energy generation for development multifunctional nanomaterials. Nanostructured multiphase materials could be conformed to obtain multi-functionality, because various characteristics of different materials can be combined to develop a wide range of fascinating features [1-8]. Efficiency and performance of products are enhanced using engineering of the interfaces in multiphase materials. The combination of functional polymers and surface alteration of nanoparticles is a vibrant area of current attention because of their fantastic electronics, optical, magnetic and catalytic features. Surface functionalization generally requires appropriate synthetic methods that offer exact control over material features. Several methods have been developed to modify nanoparticles by polymers which significantly improved their mechanical properties [9-21].

Nowadays, surface-initiated atom transfer radical polymerization (SI-ATRP) technique is recognized as a potential and flexible methods for effective grafting of accurately identified polymers, star polymers, block copolymers, graft copolymer and hyperbranched polymers from a variety of solid surfaces [22-32]. The key advantage of this technique is the complete control over the molecular weight (M_n, M_w), polydispersity (PDI) and chain-end functionality of grafted polymer. It also provides high graft density of polymer allowing multifunctional applications. Moreover, the ATRP is a widely practiced method now that it does not ask to required conditions and is accepting of functional species and contaminants that are harmful to another "living" polymerization techniques.

Recently, synthesis of polymer grafted hybrid nanoparticles having reactive pendant functionalities, such as hydroxyl, carboxylic acid or epoxide groups, has gained substantial interest as building blocks for the fabrication of advanced nanostructured devices. Biocompatible poly(2-hydroxyethyl methacrylate) is an intriguing material for biology and medicine fields as in medication carrier, dental, contact lenses, antithrombotic equipment and soft-tissue replacement. The essential features of poly(2-hydroxyethylmethacrylate) (PHEMA) such as mechanical features, thermal steady, colloidal steady, moisture content and affinity to specific biological molecules can be

adjusted to response with new requests. The features of PHEMA can be adjusted by the combination of nanomaterials and commanded by controlling the ingredient of inorganic or organic components, nanotexture, essence of inorganic and/or organic segments, *etc*. [33-37].

Among inorganic nanoparticles, silica spheres (SiO_2 nanoparticles) have excellent mechanical strength and thermal stability. They are also non-toxic, easy to functionalize and can be created controllably by hydrolysis of organosilicate at room temperature, which makes them one of the most commonly used inorganic cores. Consequently, polymers graft silica nanocomposites have received considerable attention in recent years because of high demand for optical equipment, strengthened elastomers and plastics, bioactive glass, chemical sensors, biology and medicine sensors and other types [38-40].

In this work, the exploration of an effortless and efficient procedure for precise surface alteration of SiO_2 nanoparticles with poly(2-hydroxyethylmethacrylate) (PHEMA) will not only reveal the surface properties of nanoparticles but also open up new prospects for versatile applications. We demonstrate a facile strategy for the preparation of clear identified SiO_2/PHEMA nanocomposites *via* SI-ATRP. The macroinitiator (SiO_2-Br) was first prepared by one step reaction using 3-glycidyloxypropyltrimethoxysilane (GOTMS) and 2-bromo-2-methylpropionic acid (BMPA). To obtain PHEMA-*g*-SiO_2 core-shell type nanocomposites, the surface of SiO_2 nanoparticles is modified by surface-initiated atom transfer radical polymerization of 2-hydroxyethylmethacrylate (HEMA).

EXPERIMENTAL

The SiO_2 nanoparticles with the mean size of 108 nm were prepared using Stöber technique [41] with surface area of *ca*. 115 m^2/g as measured by BET method. Purified 2-hydroxyethyl methacrylate (HEMA) was produced before hand by flowing a neutral alumina column to evict the inhibitor. NH_4OH (25 wt. % aqueous solution), tetraoctylammonium bromide (TOAB), tetraethylorthosilicate (TEOS), 3-glycidyloxypropyltrimethoxysilane (GOTMS), 2-bromo-2-methylpropanoic acid (BMPA), triethylamine (TEA), N,N,N′,N′,N″-pentamethyldiethylenetriamine (PMDETA), CuBr, tetrahydrofuran (THF), N,N-dimethylformamide (DMF) and all solvents were used as introduced.

Synthesis of strategic initiator (GOTMS-BMPA): 3-Glycidyloxypropyltrimethoxysilane (GOTMS) (2.00 g), 2-bromo-2-methylpropanoic acid (BMPA) (1.42 g) and THF (6 mL) were placed in a pyrex tube. The pipe was emptied and back-filled with nitrogen three times, then secured and held in a thermostatically with the oil bath at 70 ºC and stirred very quickly under N_2 atmosphere for 1 day. Lastly, all volatile materials was removed under vacuum and marked as GOTMS-BMPA. The ^1H NMR spectrum of GOTMS-BMPA ($CDCl_3$, 400 MHz, ppm): δ = 4.15 (CH_2-CH(OH)-CH_2-O-CO-, 2H, dd); 3.67-3.71 (CH_2-CH(OH)-CH_2-O-CO-, 1H, m); 3.62 (CH_2-CH(OH)-CH_2-O-CO-, 2H, d); 3.53 ($(CH_3O)_3Si$-, 9H, s); 3.45-3.47 (CH_2O-$(CH_2)_3Si$-, 2H, t); 1.91 (-$(CH_3)_2$-Br, 6H, s); 1.90 (CH_2-CH(OH)-CH_2-O-CO-, 1H, d); 1.67 ($SiCH_2CH_2CH_2O$, 2H, quint); 0.65 ($SiCH_2CH_2CH_2O$, 2H, d).

Synthesis of PHEMA-*g*-SiO_2 nanocomposites *via* SI-ATRP technique

Synthesis of SiO_2-Br macroinitiators: Dissolved 2.0 g of SiO_2 nanoparticles in 20 mL toluene and then added 1.0 g GOTMS-BMPA and 5 mL triethylamine (TEA) to create a uniform suspension solution. Then, the mixture was strongly stirred at 50 ºC under N_2 flow for 1 day and subsequently, cooled down to 35 ºC and cleaned in the order with toluene and dichloromethane. Next, the macroinitiator SiO_2-Br was dried at 40 ºC under vacuum for 1 day.

Synthesis of PHEMA-*g*-SiO_2 nanocomposites by SI-ATRP method: Mixed 2-hydroxyethylmethacrylate (HEMA, 2 g), SiO_2-Br (0.2 g), PMDETA (0.024 mL), CuBr (0.0166 g) in 2 mL of THF using a Teflon-covered propulsion rod in a 25 mL circle bottle decorated with a restore condenser. The mixture was removed the gas with N_2 by three freeze-pump-thaw cycles and held in an oil tank with the temperature of 80 ºC and stirred constantly. Then, the bottle was cooled to 35 ºC. Next, diethyl ether was used to precipitate the mixture and the product was separated with centrifugation. The crude product was cleaned and had impurities removed using THF multiple times. Lastly, a vacuum oven was used to dry PHEMA-*g*-SiO_2 nanocomposites for a duration of 1 night at 40 ºC. The synthetic route for SI-ATRP technique to prepare PHEMA-*g*-SiO_2 using SiO_2-Br macroinitiators is depicted in **Scheme-I**.

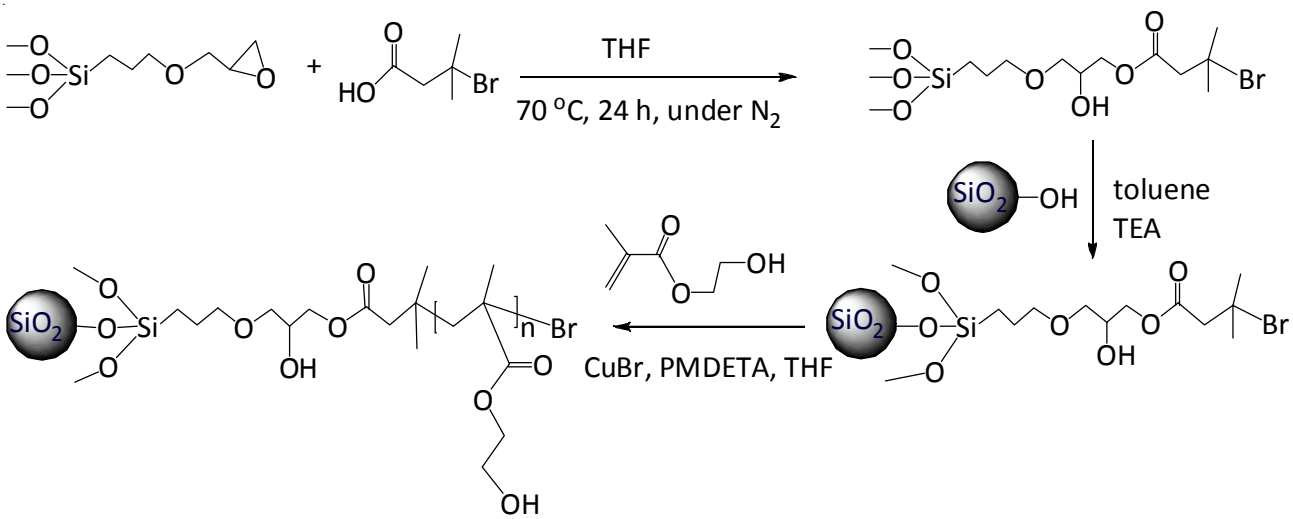

Scheme-I: Synthetic protocol for the preparation of PHEMA-*g*-SiO_2 nanocomposites *via* SI-ATRP technique

Characterizations: BOMEM Hartman & Braun spectrometer was used to determine FT-IR. Elemental analysis and morphological analysis of the hybrids was performed using FE-SEM photos attached with an EDX spectrometer (Hitachi JEOL- JSM-6700F). For TGA, Perkin-Elmer Pyris 1 analyzer (USA) was utilized. The DSC measurements were conducted using a Perkin Elmer calorimeter (DSC6200). Surface composition of nanocomposites was investigated using XPS (X-ray photoelectron spectroscopy) (Thermo VG Multilab 2000). GPC (gel permeation chromatography) analysis was performed using an Agilent 1200 Series equipped with PLgel 5 μm MIXED-C columns, with N,N-dimethylformamide at 30 ºC and calibration was performed by PMMA standards. The zeta potential for the surface charge properties of samples was carried out using a Zeta Plus 90 analyzer.

RESULTS AND DISCUSSION

The strategic initiators (GOTMS-BMPA) were attached on the surface of SiO_2 nanoparticles in one step through ligand-exchanging response among the -OH species on the surface of SiO_2 nanoparticles and trimethoxyliane groups of GOTMS-BMPA to produce SiO_2-Br macroinitiators. Fig. 1 showed the surface chemical composition of functionalized SiO_2 nanoparticles through EDS and XPS analyses. The EDX scan revealed the attendance of Si, O and C chemical components in SiO_2 nanoparticles as displayed in Fig. 1A. Fig. 1C showed that signals of Si, O and C elements affected the vast-scan XPS spectrum of SiO_2 nanoparticles surface. GOTMS-BMPA was attached on the surface of SiO_2 nanoparticles that causes a condensation response to form a stable initiator monolayer. Fig. 1B showed that clear signal of bromine atoms on surfaces of SiO_2-Br macroinitiators *via* EDS analysis. To assert the presence of ATRP initiators on SiO_2 nano-surfaces, SiO_2-Br macroinitiators was also analyzed XPS as shown in Fig. 1D. Expectedly, in the scan, we found that the primary peak component, nominated to O1s, and the small peak component, nominated to C1s, at the binding energy are of 533.6 and 285.0 eV, respectively. In addition to this, peaks at the binding energy of 154.8 eV (Si2s) and 103.7 eV (Si2p) were also found. In particular, the characteristic Br3d peak as sighted at 69.2 eV, which verifies the presence of Br signals on SiO_2 nanoparticles surfaces. The EDS and XPS results confirm the success of the formation of SiO_2-Br macroinitiators.

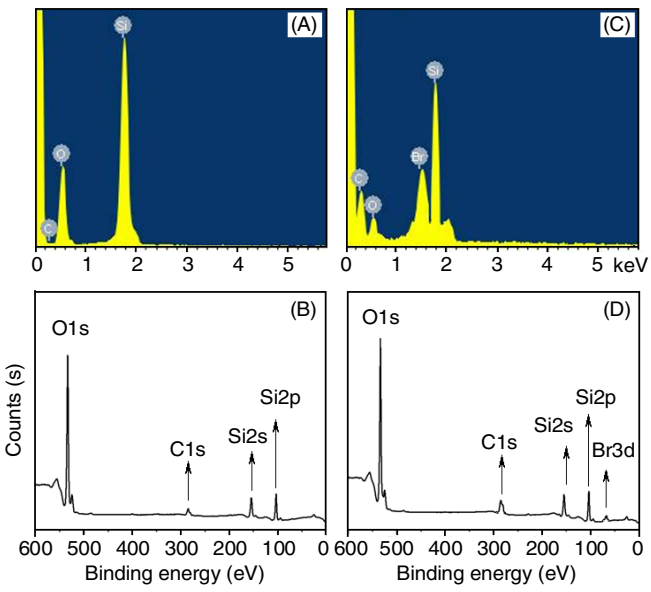

Fig. 1. (A, B) EDS and (C, D) XPS wide-scan spectra of (A, C) the SiO_2 NPs, (B, D) SiO_2-Br macroinitiators

The FT-IR was used to study the surface chemical bonding of modified SiO_2 nanoparticles. Characteristically, asymmetric stretching of Si-O-Si is associated to the absorption band, detected at 1104 cm^{-1}. The broad absorption band centered around 3431 cm^{-1} is assigned to -OH species on the surface of SiO_2 nanoparticles (Fig. 2A). Four absorption bands at 2920 cm^{-1} (C-H stretching of $-CH_3$), 2851 cm^{-1} (C-H stretching of $=CH_2$), 1737 cm^{-1} (C=O stretching) and 1114 cm^{-1} (Si-O-Si stretching which overlapped C-O-C stretching) (Fig. 2B) indicated the interaction between GOTMS-BMPA and the surface-bound OH groups of SiO_2 nanoparticles. The surface initiated ATRP of HEMA from GOTMS-BMPA enclosed SiO_2 nanoparticles surface was performed in the attendance of CuBr/PMDETA catalyst system to give PHEMA-*g*-SiO_2 nanocomposites. The successful synthesis of core-shell textured PHEMA-*g*-SiO_2 nanocomposites was verified by respective spectral and microanalyses. Fig. 2C displayed FT-IR spectrum of PHEMA-*g*-SiO_2, the broad absorption band at 3647-3022 cm^{-1} is assigned for the O-H stretching vibration and growth in intensity at 2936, 2851 cm^{-1} is due to the C-H stretching vibration. The characteristic absorption band appeared at 1725 cm^{-1} shows C=O stretching vibration band. The typical bands at 1225-1180 cm^{-1} assigned for the stretching of -C-O- (in ester species). The wide absorption bands at 800-500 cm^{-1} assigned for Si-O-Si stretching which is generally frequent in SiO_2 associated forms, and the band sighted at 1634 cm^{-1} indicates the attendance of physically adsorbed aqua in the SiO_2 forms. FT-IR analyses suggested that PHEMA was covalently attached with SiO_2 nanoparticles *via* SI-ATRP.

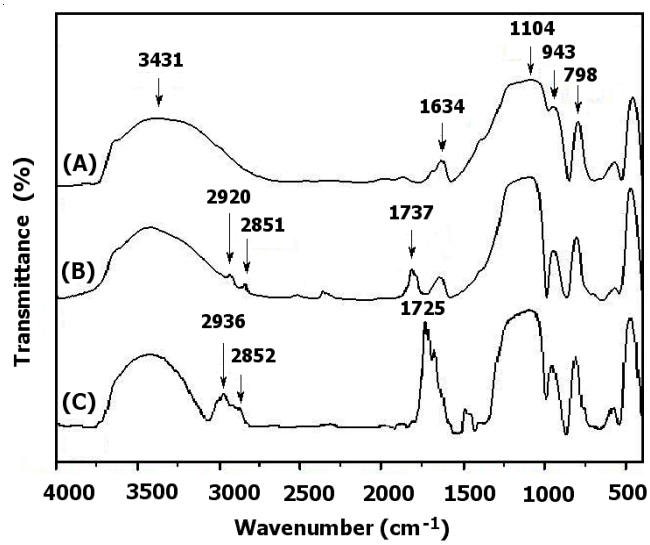

Fig. 2. FT-IR spectra of (A) SiO_2 NPs, (B) SiO_2-Br macroinitiators, (C) PHEMA-*g*-SiO_2 nanocomposites

Fig. 3 showed the results of thermogravimetric analysis from which the number of organic components anchored to SiO_2 nanoparticles is determined. From TGA analysis, the initial and final depravity temperature of the samples were determined.

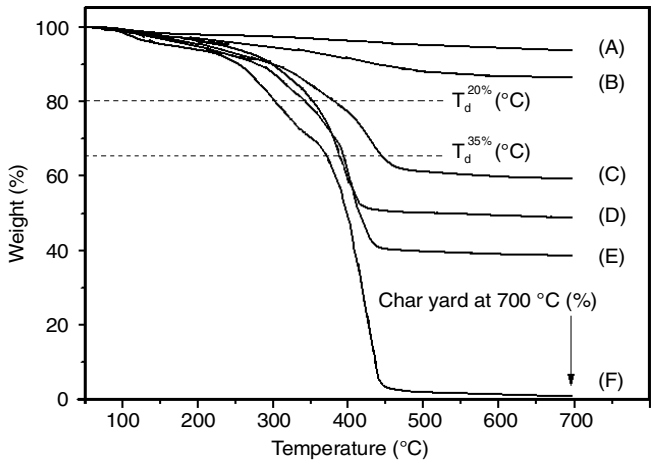

Fig. 3. TGA scans of (A) SiO_2 NPs, (B) SiO_2–Br macroinitiators, PHEMA-*g*-SiO_2 after polymerization for (C) 8 h, (D) 16 h, and (E) 24 h and (F) cleaved PHEMA from PHEMA-*g*-SiO_2 nanocomposites

Visually, by increasing the temperature from 50 to 700 ºC, the sample of SiO_2 nanoparticles loses approximately 5.1 % of their total weight. This is due to the removal of aqua molecules adsorbed on the outer and the liberation of textured aqua caused by the bonded -OH species. Thermogravimetric analysis (Fig. 3) shows that the amount of grafted GOTMS-BMPA was calculated as to be *ca*. 10.7 %. In temperature region from 285 to 430 ºC, PHEMA-*g*-SiO_2 nanocomposites were decomposed, which is basically because of the breakdown of grafted PHEMA on SiO_2 nanoparticles. It is sighted that the weight decline of nanocomposites changed from 40.2 to 61.2 % based on the polymerization time from 8 to 24 h. The results suggested a reasonable level of functionalization of SiO_2 nanoparticles by PHEMA.

The condition in which SI-ATRP polymerization occurred and molecular weight of grafted PHEMA were determined by separating the grafted polymers from PHEMA-*g*-SiO_2 nanocomposites using HF aqueous solution. The GPC analysis was performed to determine M_n and PDI of separated PHEMA. In Fig. 4, M_n and PDI of grafted PHEMA was plotted in the two vertical axes and the overall monomer conversions were displayed in the horizontal axis. The M_n of PHEMA was found to be proportional with increasing monomer conversion. The cleaved PHEMA

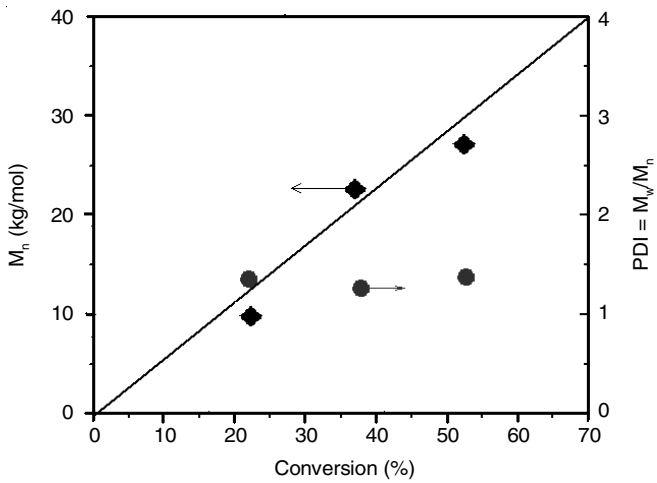

Fig. 4. M_n and PDI of the cleaved PHEMA from PHEMA-*g*-SiO_2 nanocomposites at different polymerization time (8, 16 and 24 h)

at polymerization time of 8, 16 and 24 h resulted in M_n of 10.5, 22.7 and 27.8 kg/mol with relatively narrow PDI of 1.37, 1.26 and 1.41, respectively, suggesting that SI-ATRP of HEMA from SiO_2 nanoparticles surface took place in a controlled way.

Thermal property of separated PHEMA and PHEMA-*g*-SiO_2 nanocomposites was further examined by DSC. The glass transition temperature (T_g) of cleaved PHEMA is observed at 90.4 ºC. On the other hand, the T_g of nanocomposites at polymerization time of 8, 16 and 24 h were found to be 98.2, 106.6 and 112.4 ºC, respectively. It was observed that T_g of PHEMA-*g*-SiO_2 enhanced by the high grafting of PHEMA. The T_g value of grafted PHEMA is higher by *ca*. 8-20 ºC than that of the equivalent neat PHEMA form (Fig. 5). The increase of T_g can be explained in such a way that the confinement of one head of PHEMA series on SiO_2 nanoparticles would limit both the motion and vibration of whole series that eventually happened in strong interaction as well as inherent high modulus of SiO_2 nanoparticles resulted in increased T_g.

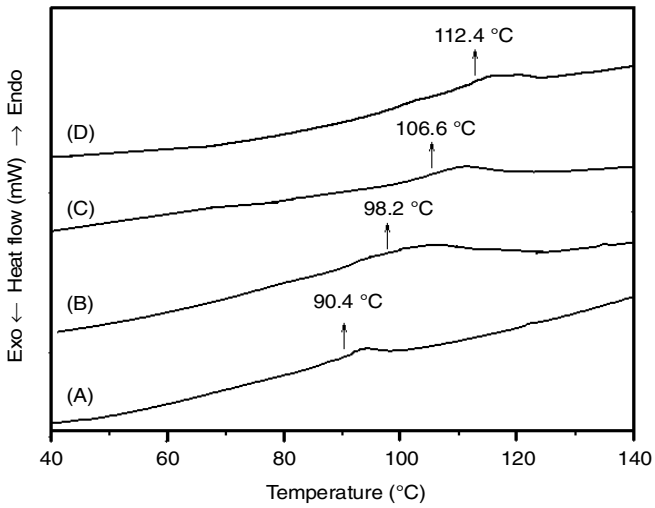

Fig. 5. DSC curves of (A) cleaved PHEMA, PHEMA-*g*-SiO_2 nanocomposites at polymerization time of (B) 8 h, (C) 16 h and (D) 24 h, respectively

The electrical property of particles surfaces regarding the zeta potential (ζ) is an essential factor for applications in biomedical, industrial and environmental areas. The ζ of modified SiO_2 nanoparticles in suspension was determined using a Brookhaven Zeta Plus 90 analyzer. All the dispersions were adjusted to the desired pH with HCl (0.25 M) and NaOH (0.25 M). ζ vs pH bends for SiO_2 nanoparticles and PHEMA-*g*-SiO_2 nanocomposites are plotted (Fig. 6). For SiO_2 nanoparticles, negative zeta voltage was found all the whole examined pH region. The surface charge density of SiO_2 nanoparticles suspensions was observed to be decreased as the pH of suspension was increased and the isoelectric point (p*I*) was reached around at pH 3.0. In opposition, ζ *vs*. pH bends for the PHEMA- *g*-SiO_2 nanocomposites indicated the survival of p*I* at *ca*. pH = 6 and positive zeta voltage of situated above to + 40 mV was attained at low pH. So, this results given proof that the covalent modification of SiO_2 nanoparticles by PHEMA significantly increased the surface charge behavior of unmodified SiO_2 nanoparticles which can be used as a non-viral vector for transferring genetic materials (gene, DNA, RNA) across cellular membranes.

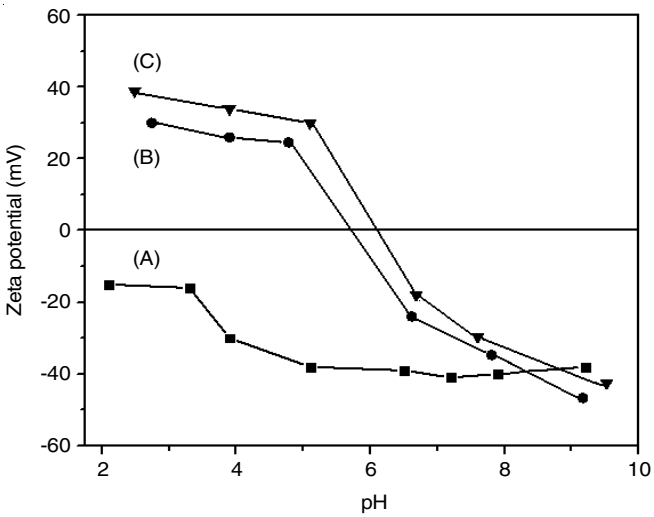

Fig. 6. Zeta potential *vs.* pH curves for (A) SiO_2 NPs and PHEMA-*g*-SiO_2 at polymerization time of (B) 8 h and (C) 24 h, respectively

Conclusion

Surface modification of SiO_2 nanoparticles by poly(2-hydroxyethylmethacrylate (PHEMA) was accomplished to afford PHEMA-*g*-SiO_2 nanocomposites *via* a facile SI-ATRP method. Following the anchoring of a sacrificial initiator GOTMS-BMPA to the surface of SiO_2 nanoparticles, chemically bonded PHEMA-*g*-SiO_2 nanocomposites were synthesized by SI-ATRP of 2-hydroxyethylmethacrylate (HEMA) from the surface of SiO_2 nanoparticles employing grafting from strategy as confirmed by FT-IR analyses. The thermal steady of grafted PHEMA was dramatically improved compared to pure PHEMA as suggested by TGA and DSC studies. The controlled nature of polymerization was evidenced by the linear increase of M_n of the separated PHEMA from PHEMA-*g*-TiO_2 nanocompo-sites with monomer conversion and the relatively low PDI (< 1.5). The zeta potential of functionalized SiO_2 nanoparticles indicated that surface modification by PHEMA using SI-ATRP is a fantastic strategy for manipulating surface electrostatic character of SiO_2 nanoparticles. This facile chemical strategy holds a great promise for surface engineering of nanoparticles in material science and nanotechnology to devise a cascade of promising materials for diverse applications.

ACKNOWLEDGEMENTS

This work was supported by Nguyen Tat Thanh University, Vietnam.

CONFLICT OF INTEREST

The authors declare that there is no conflict of interests regarding the publication of this article.

REFERENCES

1. M. Dabrowski, P. Lach, M. Cieplak and W. Kutner, *Biosens. Bioelectron.*, **102**, 17 (2018); https://doi.org/10.1016/j.bios.2017.10.045.
2. L. Peponi, D. Puglia, L. Torre, L. Valentini and J.M. Kenny, *Mater. Sci. Eng. Rep.*, **85**, 1 (2014); https://doi.org/10.1016/j.mser.2014.08.002.
3. M. Wang, X. Wang, M. Chen, Z. Yang and C. Dong, *Chin. J. Catal.*, **37**, 1037 (2016); https://doi.org/10.1016/S1872-2067(16)62477-4.
4. W. Salim and W.S.W. Ho, *Curr. Opin. Chem. Eng.*, **8**, 76 (2015); https://doi.org/10.1016/j.coche.2015.03.003.
5. J. Song and J. Jang, *Adv. Colloid Interface Sci.*, **203**, 37 (2014); https://doi.org/10.1016/j.cis.2013.11.007.
6. M. Mir, N. Ahmed and A. Rehman, *Colloids Surf. B Biointerfaces*, **159**, 217 (2017); https://doi.org/10.1016/j.colsurfb.2017.07.038.
7. S. Kassim and M. Pemble, *Asian J. Chem.*, **30**, 1617 (2018); https://doi.org/10.14233/ajchem.2018.21280.
8. M. Santhiago, P.S. Garcia and M. Strauss, *Curr. Opin. Green Sustain. Chem.*, **12**, 22 (2018); https://doi.org/10.1016/j.cogsc.2018.04.009.
9. L.G. Bach, X.T. Cao, M.R. Islam, H.G. Kim and K.T. Lim, *J. Nanosci. Nanotechnol.*, **15**, 5897 (2015); https://doi.org/10.1166/jnn.2015.10438.
10. L.G. Bach, X.T. Cao, V.T.T. Ho, M.R. Islam and K.T. Lim, *Mol. Cryst. Liq. Cryst.*, **618**, 120 (2015); https://doi.org/10.1080/15421406.2015.1076315.
11. X.T. Cao, L.G. Bach, M.R. Islam and K.T. Lim, *Mol. Cryst. Liq. Cryst.*, **618**, 111 (2015); https://doi.org/10.1080/15421406.2015.1076305.
12. L.G. Bach, B.T.P. Quynh, M.R. Islam and K.T. Lim, *J. Nanosci. Nanotechnol.*, **16**, 12856 (2016); https://doi.org/10.1166/jnn.2016.13651.
13. L.G. Bach, X.T. Cao, B.T.P. Quynh, V.T.T. Ho and K.T. Lim, *Mol. Cryst. Liq. Cryst.*, **644**, 183 (2017); https://doi.org/10.1080/15421406.2016.1277478.
14. L.G. Bach, B.T.P. Quynh, N.T. Thuong and V.T.T. Ho, *Mol. Cryst. Liq. Cryst.*, **644**, 175 (2017); https://doi.org/10.1080/15421406.2016.1277476.
15. L.G. Bach, B.T.P. Quynh and V.T.T. Ho, *J. Nanosci. Nanotechnol.*, **17**, 4127 (2017); https://doi.org/10.1166/jnn.2017.13381.
16. C. Leopold, T. Augustin, T. Schwebler, J. Lehmann, W.V. Liebig and B. Fiedler, *J. Colloid Interface Sci.*, **506**, 620 (2017); https://doi.org/10.1016/j.jcis.2017.07.085.
17. G. Yang, X. Li, Y. He, J. Ma, G. Ni and S. Zhou, *Prog. Polym. Sci.*, **81**, 80 (2018); https://doi.org/10.1016/j.progpolymsci.2017.12.003.
18. S. Mallakpour and E. Khadem, *Prog. Polym. Sci.*, **51**, 74 (2015); https://doi.org/10.1016/j.progpolymsci.2015.07.004.
19. S. Agbolaghi, S. Abbaspoor and F. Abbasi, *Prog. Polym. Sci.*, **81**, 22 (2018); https://doi.org/10.1016/j.progpolymsci.2017.11.006.
20. A. Sosnik, J. das Neves and B. Sarmento, *Prog. Polym. Sci.*, **39**, 2030 (2014); https://doi.org/10.1016/j.progpolymsci.2014.07.010.
21. S. Kumar, M. Sarita, M. Nehra, N. Dilbaghi, K. Tankeshwar and K.-H. Kim, *Prog. Polym. Sci.*, **80**, 1 (2018); https://doi.org/10.1016/j.progpolymsci.2018.03.001.
22. Y. Zhao, L. Wang, A. Xiao and H. Yu, *Prog. Polym. Sci.*, **35**, 1195 (2010); https://doi.org/10.1016/j.progpolymsci.2010.05.002.
23. P. Krys and K. Matyjaszewski, *Eur. Polym. J.*, **89**, 482 (2017); https://doi.org/10.1016/j.eurpolymj.2017.02.034.
24. J. Ran, L. Wu, Z. Zhang and T. Xu, *Prog. Polym. Sci.*, **39**, 124 (2014); https://doi.org/10.1016/j.progpolymsci.2013.09.001.
25. F. Seidi, H. Salimi, A.A. Shamsabadi and M. Shabanian, *Prog. Polym. Sci.*, **76**, 1 (2018); https://doi.org/10.1016/j.progpolymsci.2017.07.006.
26. P. Król and P. Chmielarz, *Prog. Org. Coat.*, **77**, 913 (2014); https://doi.org/10.1016/j.porgcoat.2014.01.027.
27. Y. Liu and C.E. Hobbs, *Polymer*, **135**, 25 (2018); https://doi.org/10.1016/j.polymer.2017.12.001.
28. P. Polanowski, K. Halagan, J. Pietrasik, J.K. Jeszka and K. Matyjaszewski, *Polymer*, **130**, 267 (2017); https://doi.org/10.1016/j.polymer.2017.10.011.
29. J.M. Kubiak, J. Yan, J. Pietrasik and K. Matyjaszewski, *Polymer*, **117**, 48 (2017); https://doi.org/10.1016/j.polymer.2017.04.012.

30. M. Chen, L. Qin, Y. Liu and F. Zhang, *Microporous Mesoporous Mater.*, **263**, 158 (2018); https://doi.org/10.1016/j.micromeso.2017.12.019.
31. L. Huang, M. Liu, L. Mao, D. Xu, Q. Wan, G. Zeng, Y. Shi, Y. Wen, X. Zhang and Y. Wei, *Appl. Surf. Sci.*, **412**, 571 (2017); https://doi.org/10.1016/j.apsusc.2017.04.026.
32. S. Kumar, P. Karfa, R. Madhuri and P.K. Sharma, *J. Phys. Chem. Solids*, **116**, 222 (2018); https://doi.org/10.1016/j.jpcs.2018.01.038.
33. M. Kubo, T. Kondo, H. Matsui, N. Shibasaki-Kitakawa and T. Yonemoto, *Ultrason. Sonochem.*, **40**, 736 (2018); https://doi.org/10.1016/j.ultsonch.2017.08.011.
34. Z. Sadakbayeva, M. Dušková-Smrcková, A. Šturcová, J. Pfleger and K. Dušek, *Eur. Polym. J.*, **101**, 304 (2018); https://doi.org/10.1016/j.eurpolymj.2018.02.035.
35. V.V. Filipovic, B.Đ. Bozic Nedeljkovic, M. Vukomanovic and S.L. Tomic, *Polym. Test.*, **68**, 270 (2018); https://doi.org/10.1016/j.polymertesting.2018.04.024.
36. S. Sundararajan, A.B. Samui and P.S. Kulkarni, *React. Funct. Polym.*, **130**, 43 (2018); https://doi.org/10.1016/j.reactfunctpolym.2018.05.012.
37. S. Wu, W. Du, Y. Duan, D. Zhang, Y. Liu, B. Wu, X. Zou, H. Ouyang and C. Gao, *Acta Biomater.*, **75**, 75 (2018); https://doi.org/10.1016/j.actbio.2018.05.046.
38. H. Chen, X. Zhang, P. Zhang and Z. Zhang, *Appl. Surf. Sci.*, **261**, 628 (2012); https://doi.org/10.1016/j.apsusc.2012.08.071.
39. S. Mallakpour and M. Naghdi, *Prog. Mater. Sci.*, **97**, 409 (2018); https://doi.org/10.1016/j.pmatsci.2018.04.002.
40. Sh. Ammar, K. Ramesh, I.A.W. Ma, Z. Farah, B. Vengadaesvaran, S. Ramesh and A.K. Arof, *Surf. Coat. Technol.*, **324**, 536 (2017); https://doi.org/10.1016/j.surfcoat.2017.06.014.
41. L.G. Bach, M.R. Islam, Y.T. Jeong, H.S. Hwang and K.T. Lim, *Mol. Cryst. Liq. Cryst.*, **565**, 78 (2012); https://doi.org/10.1080/15421406.2012.692262.